Journal of NUCLEAR SCIENCE and TECHNOLOGY, Supplement 2, p. 818–821 (August 2002)

Vanishing of the $N = 20$ Magic Number Studied by the Monte Carlo Shell Model

Yutaka UTSUNO[1,*], Takaharu OTSUKA[2,3], Takahiro MIZUSAKI[4] and Michio HONMA[5]

[1]*Japan Atomic Energy Research Institute, Tokai Ibaraki 319-1195, Japan*
[2]*Department of Physics, University of Tokyo, Hongo, Bunkyo-ku, Tokyo 113-0033, Japan*
[3]*RIKEN, Hirosawa, Wako-shi, Saitama 351-0198, Japan*
[4]*Institute of Natural Sciences, Senshu University, Higashimita, Tama, Kawasaki, Kanagawa 214-8580, Japan*
[5]*Center for Mathematical Sciences, University of Aizu, Tsuruga, Ikki-machi Aizu-Wakamatsu, Fukushima 965-8580, Japan*

The structure of unstable nuclei around $N = 20$ is studied theoretically by the Monte Carlo shell model (MCSM). We focus mainly upon the vanishing of the $N = 20$ magic structure in this region. The binding energies, the energy levels, and the $B(E2)$ values are well reproduced by the MCSM, and some of them are predicted successfully. We discuss the mechanism of the vanishing in terms of the effective single-particle energy, pointing out that the strong $T = 0$ monopole interaction between the $0d_{5/2}$ and $0d_{3/2}$ plays an important role on the vanishing of the $N = 20$ magic number and the appearance of the new $N = 16$ one. The location of F drip line is discussed along the lines.

KEYWORDS: nuclear structure, unstable nuclei, shell model, Monte Carlo method, magic number, energy level, $B(E2)$, drip line

I. Introduction

Recently, studies on the structure and the reaction of exotic nuclei have been advanced very rapidly, showing their unique features compared to those of stable ones. One of the most intriguing issues is the change of the shell structure from stable to unstable nuclei which can give rise to the vanishing of known magic numbers and the appearance of new ones. The origin of the magic numbers has been regarded as large spherical shell gaps whose single-particle energies are obtained from the harmonic oscillator potential with the spin-orbit interaction.[1)] The magic number should remain unchanged independently of the proton and the neutron numbers in this picture, whereas anomalous ground-state properties of ^{31}Na, i.e, the binding energy,[2)] the spin, and the magnetic moment[3)] in contradiction to the *sd*-shell model, imply that the $N = 20$ magic structure vanishes for this nucleus. A low 2_1^+ energy level[4)] and a large $B(E2; 0_1^+ \rightarrow 2_1^+)$ value[5)] of ^{32}Mg clearly show the contradiction to the spherical ground state as a result of the $N = 20$ magic structure, too.

In the present paper, we systematically study the structure of unstable nuclei in the framework of large-scale shell-model calculations. To describe the vanishing of the magic structure of $N = 20$, a very large valence shell consisting of not only the full *sd* shell but also at least part of the *pf* shell should be adopted. It is still impossible to diagonalize exactly the Hamiltonian matrix with such a large model space. Therefore, in previous shell-model calculations,[6–9)] the model space is restricted to allow only up to 2-particle 2-hole excitations across the $N = 20$ shell gap. Associated with this restriction, some calculations do not take into account the mixing between the *intruder* configurations with such excitations and the *normal* ones without them. In terms of the shell model without the mixing, the vanishing of the magic number is often discussed in reference to the *island of inversion*[6)] constituting a small region of the nuclear chart where the intruder state is lower than the normal one.

The Monte Carlo shell model (MCSM)[10–13)] has been recently developed in order to overcome the difficulty of the shell-model calculation with huge dimension of the Hilbert space, and is adopted in the present study. In the MCSM calculation, candidates of the many-body basis vectors are generated stochastically according to the auxiliary Monte Carlo technique, and the most important ones among them are selected with the diagonalization of the Hamiltonian matrix. The MCSM is thus characterized as the shell model with *importance truncation.*[14)]

We can examine whether the *island of inversion* picture is really relevant or not using the MCSM, in which the mixing among the normal, intruder, and higher intruder configurations are mixed in a natural way. The mechanism of the vanishing of the magic number will be discussed. We will point out that the spherical shell structure, which is defined in the framework of the shell model by the monopole interaction, should vary as the number of nucleons increases. The vanishing of the $N = 20$ magic number and the appearance of the $N = 16$ magic number are understood in a unified picture based on a very strongly attractive monopole interaction connecting particular orbits.

II. Effective Interaction

1. Construction of the Interaction

The effective interaction used in this study is based on a combination of the USD interaction[15)] for the *sd* shell, the Kuo-Brown interaction[16)] for the *pf* shell, and the Millener-Kurath interaction with some modifications[17)] for the cross shell. This interaction with bare single-particle energies adjusted at ^{17}O and ^{41}Ca gives good properties for stable nuclei but fails to reproduce the single-particle structure of neutron-rich O isotopes. Namely, the last bound oxygen isotope is ^{24}O with $N = 16$ experimentally, whereas this interaction predicts that ^{26}O is also stable against the particle emission. This contradiction about the particle stability is owing to the

* Corresponding author, Tel. +81-29-282-5796, Fax. +81-29-282-5458, E-mail: utsuno@jball4.tokai.jaeri.go.jp

single-particle binding property of the $0d_{3/2}$ orbit: the above-mentioned interaction gives too bound $0d_{3/2}$ orbit for large N. Considering that the $0d_{3/2}$ is unbound for the ^{16}O core, we attribute this bound property to the two-body interaction between valence nucleons.

Among various matrix elements of the two-body interaction, the so-called monopole interaction[18] is responsible for the binding property. The monopole interaction between the i and the j orbits, V_{ij}^T, is defined with diagonal two-body interactions $\langle ij|V|ij\rangle_{JT}$ by

$$V_{ij}^T = \frac{\sum_J (2J+1)\langle ij|V|ij\rangle_{JT}}{\sum_J (2J+1)}, \quad (1)$$

where J and T are the angular momentum and the isospin coupled to nucleons in i and j orbits, respectively. As the angular dependence is averaged out in Eq. (1), the monopole interaction represents a mean effect between these orbits.

We shift the monopole interaction from the original interaction as

$$\begin{aligned} \delta V^{T=1,0}_{0d_{5/2},0d_{3/2}} &= +0.30, -0.70 \text{ MeV}, \\ \delta V^{T=1,0}_{0d_{5/2},0f_{7/2}} &= +0.16, -0.50 \text{ MeV}, \end{aligned} \quad (2)$$

where the $T=1$ part is made to cure the contradiction of the binding property concerning the $0d_{3/2}$ (and the pf shell) of O isotopes, and the corresponding $T=0$ part is to maintain good properties of $N \sim Z$ nuclei. In fact, the interaction with the modification of Eq. (2) reproduces the experimental drip line of O isotopes.

2. Effective Single-Particle Energy

We shall overview the spherical single-particle structure given by the present interaction, introducing the *effective single-particle energy* (ESPE). The ESPE represents the single-particle energy including mean effects from valence nucleons, and can vary as the number of nucleons changes. For a certain nucleus, we assume the natural occupancy, i.e., the configuration where the nucleons are occupied in the order of $0d_{5/2}$, $1s_{1/2}$, and $0d_{3/2}$. The ESPE of a designated orbit is defined by the separation energy from it with the opposite sign, using the monopole interaction for the evaluation of the two-body interaction.

Figure 1 shows the ESPE's of neutrons in going from the ^{16}O to the ^{40}Ca core. For O isotopes, the EPSE of each orbits is almost unchanged. The $N=16$ magic structure reflecting a large shell gap between the $1s_{1/2}$ and $0d_{3/2}$ survives in the neutron-rich region. Note that the large shell gap, created by the large spin-orbit splitting, is observed in the spectra of ^{17}O. This structure holds for larger N due to relatively weak $T=1$ monopole interaction. On the other hand, the $N=20$ shell gap is quite narrow. This represents the new $N=16$ magic number pointed out recently.[19]

The valence protons are increased in Fig. 1 (b). The ESPE's become lower on the whole. In particular the $0d_{3/2}$ lowers very steeply as protons occupy the $0d_{5/2}$, generating the $N=20$ magic number instead of the $N=16$ one. The resulting $N=20$ shell gap is about 3 MeV for Ne ($Z=10$), ending up with 6 MeV for Ca ($Z=20$).

The steep slope of the $0d_{3/2}$ as the proton number increases is brought about by a strongly attractive $T=0$ monopole interaction between the $0d_{5/2}$ and the $0d_{3/2}$. Recently, the origin of this strongly attractive interaction has been discussed in terms of the spin-isospin property of the nucleon-nucleon interaction.[20]

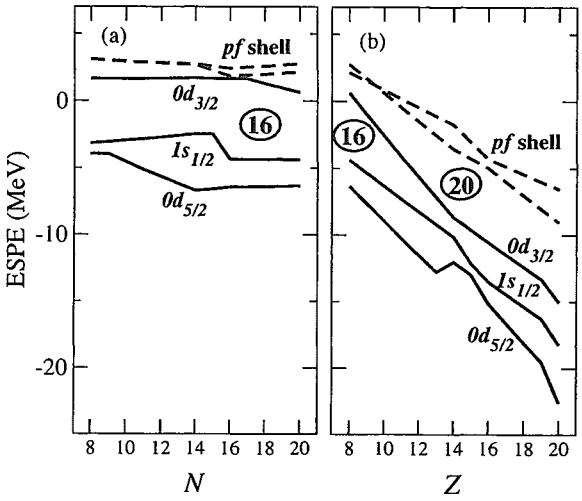

Fig. 1 Effective single-particle energies of neutrons for (a) O isotopes and (b) $N=20$ isotones.

III. Results and Discussion

We can calculate various properties of neutron-rich nuclei around $N=20$ including the binding energies, the energy levels, the electromagnetic moments and transitions, *etc.* with a single framework of the MCSM. We now discuss some of them.

1. Energy Levels and $B(E2)$ of Ne, Mg, and Si Isotopes

Figure 2 shows the yrast energy levels and the $B(E2)$ values of even-A Ne, Mg, and Si isotopes from $N=16$ to 24.[21] The results calculated by the MCSM are compared with experiment. The sd-shell calculations, assuming the $N=20$ core to be inert, are also performed with the USD interaction[15] to examine effects of configurations excited from the $N=20$ core.

For Ne and Mg with $N=20$, the results by the MCSM are quite different from the sd-shell calculations. The 2_1^+ levels are rather low compared with the other $N<20$ isotopes, and the $B(E2)$ values are enhanced in agreement with the experiments of ^{32}Mg.[4,5] The dominant configuration of the ground states of them is the 2-particle 2-hole ($2p2h$) excited one from the $N=20$ core, producing the vanishing of the $N=20$ magic structure. The $2p2h$ probability in the ground state of ^{32}Mg reaches about 85%, confirming its $2p2h$ dominance suggested in the picture of the island of inversion.[6,9]

The yrast energy levels of ^{34}Mg with $N=22$ have been measured quite recently by Yoneda *et al.*[22] The measured 2_1^+ level is located at 660 keV in excellent agreement with the MCSM prediction. The MCSM indicates that ^{34}Mg is domi-

nated by the intruder configurations. The excitation energy of the 2_1^+ calculated from the normal configurations is predicted to lie at higher than 1 MeV,[9] supporting the vanishing of the magic structure for ^{34}Mg.

The location of the boundary of the island of inversion is of interest, too. The mixing between different configurations may be important at the boundary, and the MCSM calculation is suitable for the issue. The 2_1^+ energy level of an $N=18$ nucleus ^{28}Ne is located considerably lower than the *sd*-shell prediction, while the MCSM gives good excitation energy. The MCSM shows that the $2p2h$ probability in the ground state of ^{28}Ne amounts to 56%. This strong mixing with the intruder configurations for ^{28}Ne is related most likely to the narrowing $N=20$ shell gap for smaller Z shown in Fig. 1.

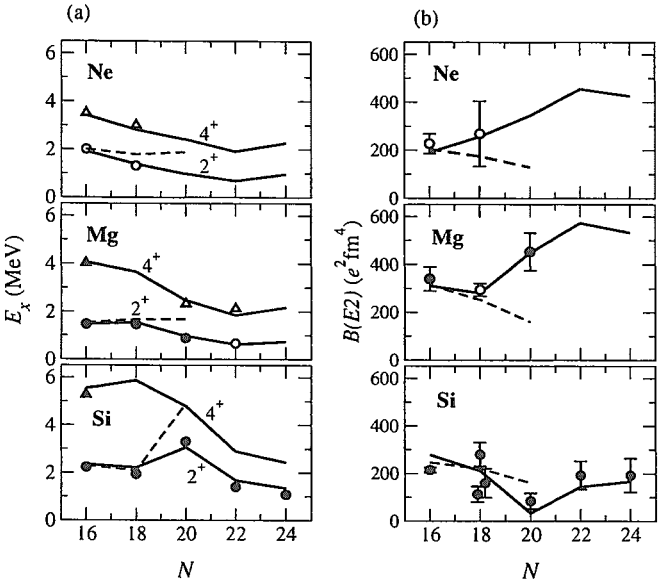

Fig. 2 (a) Energy levels and (b) $B(E2;0_1^+ \rightarrow 2_1^+)$ values of Ne, Mg, and Si isotopes. Solid and dashed lines are the MCSM and the *sd*-shell calculations, respectively. Filled and open symbols denote experimental values published before and after the MCSM calculation[21] was finished, respectively.

2. Location of the Drip Line of F Isotopes

One of the most puzzling properties of exotic nuclei in this region is the drip line of fluorine located far. Namely, the drip lines of $Z=6$ - 8 isotopes are located at $N=16$, whereas it extends quite farther at least to $N=22$ for F with $Z=9$.[24] It has been considered in the picture of the island of inversion[6,9] that ^{29}F is located outside the island, because little proton-neutron correlation energy cannot overcome the $N=20$ shell-gap energy if it is moderately large. The drip line of O isotopes can be understood in terms of the ESPE of the $0d_{3/2}$ in Fig. 1. The $0d_{3/2}$ becomes a bound orbit for F owing to the attractive monopole interaction with the $0d_{5/2}$ orbit. However, it is difficult for ^{29}F with $N=20$ to be a bound nucleus in the framework of the *sd*-shell model, since there is no correlation for the closed-shell configuration so that the energy gain in the $0d_{3/2}$ ESPE of ^{29}F cannot overcome the loss of the correlation energy which exists in ^{27}F. In fact, it was shown that ^{29}F is not a bound nucleus within the normal configuration,[9] which is confirmed with the present interaction.

In the present study, we can take into account the effect of the configurations with not only the $2p2h$'s but also the $4p4h$'s, *etc.*[25] In **Fig. 3**, the two-neutron separation energies (S_{2n}'s) of $N=20$ isotones are shown. The S_{2n}'s of $Z \geq 10$ isotones are in good agreement with the experiment. The S_{2n} of ^{29}F is a negative value in the $0p0h$ calculation as discussed already. Figure 3 indicates that the situation remains unchanged for the $0p0h + 2p2h$ calculation, too. In the full configuration, it becomes a bound nucleus at last. The ground state includes considerable contributions of the $4p4h$ configurations shown in Fig. 3 (b). The enhancement of the $4p4h$ plays a crucial role in the binding property of ^{29}F, affected much by the narrowing $N=20$ shell gap for smaller Z as illustrated in Fig. 1.

In the present calculation, ^{31}F, known to be a bound nucleus, is slightly unbound against the two-neutron emission. The contradiction may be cured by incorporating effects of the halo structure. In fact, it becomes bound by lowering the $1p_{3/2}$ single-particle energy by 350 keV.

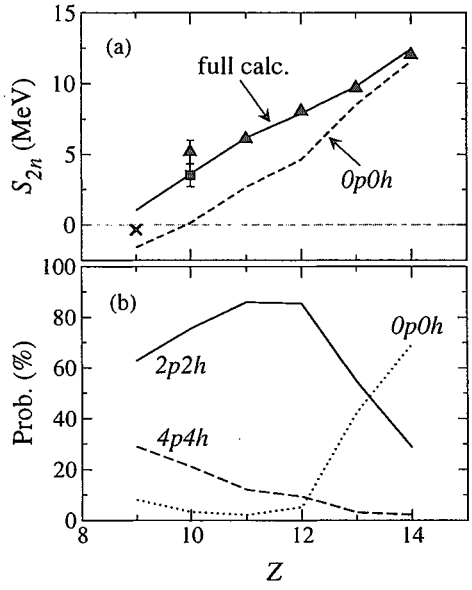

Fig. 3 (a) Two-neutron separation energies and (b) $npnh$ ($n=0,2,4$) probabilities in the ground states of $N=20$ isotones. The square in (a) is a recent datum.[23] The cross in (a) corresponds to the $0p0h + 2p2h$ calculation with the present interaction.

IV. Summary

The structure of neutron-rich nuclei around $N=20$ has been systematically studied with the MCSM calculations. The varying single-particle properties of neutron-rich nuclei are carefully treated in constructing the effective interaction. The behavior of the $0d_{3/2}$ orbit in neutron-rich nuclei plays an important role on the vanishing of the $N=20$ magic number, reflecting a strongly attractive $T=0$ monopole interaction be-

tween the $0d_{3/2}$ and the $0d_{5/2}$. Yrast properties of even-even Ne, Mg, and Si isotopes are described very well with this framework, and we have succeeded in predicting some quantities, including very large deformation of ^{34}Mg. The location of the drip line of F has been discussed also. The narrowing $N=20$ shell gap allows the $2p2h$ intruder and higher intruder configurations to dominate the ground state. This kind of mixing remedies the contradiction of the binding property of ^{29}F in the *sd*-shell calculation. The success in the systematic description of stable and unstable nuclei with the MCSM should have much influence on the field of the nuclear data, particularly in unstable ones which are not easily accessible by experiment.

Acknowledgment

The MCSM calculations were carried out with the Alphleet Computer system in RIKEN. This work was supported in part by Grant-in-Aid for Scientific Research No. (A)(2) (10304019) from the Ministry of Education, Science and Culture.

References

1) M.G. Mayer, J.H.D. Jensen, *Elementary Theory of Nuclear Shell Structure*, Wiley, New York (1955).
2) C. Thibault, R. Klapisch, C. Rigaud *et al.*, "Direct measurement of the masses of ^{11}Li and $^{26-32}$Na with an on-line mass separator", *Phys. Rev. C* **12**, 644 (1975).
3) G. Huber, F. Touchard, S. Büttgenbach, *et al.*, "Spins, magnetic moments, and isotope shifts of $^{21-31}$Na by high resolution laser spectroscopy of the Atomic D_1 line", *Phys. Rev. C* **18**, 2342 (1978).
4) C. Détraz, D. Guillemaud, G. Huber, *et al.*, "Beta decay of $^{27-32}$Na and their descendants", *Phys. Rev. C* **19**, 164 (1979); D. Guillemaud-Mueller, C. Détraz, M. Langevin, *et al.*, "β-decay schemes of very neutron-rich sodium isotopes and their descendants", *Nucl. Phys.* **A426**, 37 (1984).
5) T. Motobayashi, Y. Ikeda, Y. Ando, *et al.*, "Large deformation of the very neutron-rich nucleus ^{32}Mg from intermediate-energy Coulomb excitation", *Phys. Lett. B* **346**, 9 (1995).
6) E.K. Warburton, J.A. Becker, B.A. Brown, "Mass systematics for $A=29$ - 44 nuclei: the deformed $A\sim32$ region", *Phys. Rev. C* **41**, 1147 (1990).
7) N. Fukunishi, T. Otsuka, T. Sebe, "Vanishing of the shell gap in $N=20$ neutron-rich nuclei, *Phys. Lett. B* **296**, 279 (1992).
8) A. Poves, J. Retamosa, "Theoretical study of the very neutron-rich nuclei around $N=20$", *Nucl. Phys.* **A571**, 221 (1994).
9) E. Caurier, F. Nowacki, A. Poves, J. Retamosa, "Shell model study of the neutron-rich isotopes from oxygen to silicon", *Phys. Rev. C* **58**, 2033 (1998).
10) M. Honma, T. Mizusaki, T. Otsuka, "Diagonalization of Hamiltonians for many-body systems by auxiliary field quantum Monte Carlo technique", *Phys. Rev. Lett.* **75**, 1284 (1995).
11) T. Mizusaki, M. Honma, T. Otsuka, "Quantum Monte Carlo diagonalization with angular momentum projection", *Phys. Rev. C* **53**, 2786 (1996).
12) M. Honma, T. Mizusaki, T. Otsuka, "Nuclear shell model by the quantum Monte Carlo diagonalization method", *Phys. Rev. Lett.* **77**, 3315 (1996).
13) T. Otsuka, M. Honma, T. Mizusaki, "Structure of the $N=Z=28$ closed shell studied by Monte Carlo shell model calculation", *Phys. Rev. Lett.* **81**, 1588 (1998).
14) T. Otsuka, T. Mizusaki, M. Honma, "Monte Carlo shell-model calculations", *J. Phys. G: Nucl. Part. Phys.* **25**, 699 (1999).
15) B.A. Brown, B.H. Wildenthal, "Status of the nuclear shell model", *Annu. Rev. Nucl. Part. Sci.* **38**, 29 (1988).
16) T.T.S. Kuo, G.E. Brown, "Reaction matrix elements for the $0f$-$1p$ shell nuclei", *Nucl. Phys.* **A114**, 241 (1968).
17) E.K. Warburton, D.E. Alburger, J.A. Becker, B.A. Brown, S. Raman, "Probe of the shell crossing at $A=40$ via beta decay: experiment and theory", *Phys. Rev. C* **34**, 1031 (1986).
18) A. Poves, A. Zuker, "Theoretical spectroscopy and the fp shell", *Phys. Rep.* **70**, 235 (1981).
19) A. Ozawa, T. Kobayashi, T. Suzuki, K. Yoshida, I. Tanihata, "New magic number, $N=16$, near the neutron drip line", *Phys. Rev. Lett.* **84**, 5493 (2000).
20) T. Otsuka, R. Fujimoto, Y. Utsuno, B.A. Brown, M. Honma, T. Mizusaki, "Magic numbers in exotic nuclei and spin-isospin properties of the NN interaction", *Phys. Rev. Lett.* **87**, 082502 (2001).
21) Y. Utsuno, T. Otsuka, T. Mizusaki, M. Honma, "Varying shell gap and deformation in $N\sim20$ unstable nuclei studied by the Monte Carlo shell model", *Phys. Rev. C* **60**, 054315 (1999).
22) K. Yoneda, H. Sakurai, T. Gomi, *et al.*, "Deformation of ^{34}Mg studied via in-beam γ-ray spectroscopy using radioactive-ion projectile fragmentation", *Phys. Lett. B* **449**, 233 (2001).
23) F. Sarazin, H. Savajols, W. Mittig, *et al.*, "Shape coexistence and the $N=28$ shell closure far from stability", *Phys. Rev. Lett.* **84**, 5062 (2000).
24) H. Sakurai, S.M. Lukyanov, M. Notani, *et al.*, "Evidence for particle stability of ^{31}F and particle instability of ^{25}N and ^{28}O", *Phys. Lett. B*, **448**, 180 (1999).
25) Y. Utsuno, T. Otsuka, T. Mizusaki, M. Honma, "Extreme location of F drip line and disappearance of the $N=20$ magic structure", *Phys. Rev. C* **64**, 011301(R) (2001).